Journal of Stress Analysis
Vol. 6, No. 2, Autumn – Winter 2021-22, 47-57
Bu-Ali Sina University

ORIGINAL RESEARCH PAPER

Numerical Study on the Effect of Biaxial Surface Stresses on the Measurement Accuracy of Mechanical Properties in A516 Using Indentation

F. Barati, R. Moharrami*
Mechanical Engineering Department, University of Zanjan, Zanjan, Iran.

Article info

Article history:
Received 25 December 2021
Received in revised form
20 January 2022
Accepted 08 February 2022

Keywords:
Mechanical properties
Surface stress
Instrumented indentation technique
Measurement accuracy

Abstract

Accuracy in determination of mechanical properties in industrial parts is a major issue in engineering. Various methods have been introduced to estimate the mechanical properties of the industrial parts, and each has its own features and limitations. The present research investigates the accuracy of Instrumented Indentation Technique (IIT) with Kim's model in determining mechanical properties, including elastic modulus, yield stress, and work hardening of the A516 steel samples having surface stresses. To this end, some 3D simulations, using IIT on the steel sample with different surface stress state, were performed, and the method's error in comparison to the initial assumed values were obtained. The results show that the surface stresses significantly affect the error in determining the materials' properties, and the error in samples with tensile surface stress is more than that of samples with compressive one. To validate the results, some experimental samples with specified initial stress were prepared, which measured mechanical properties by the IIT and then were compared with the tensile test results.

Nomenclature

A_c	Contact area, m^2	E	Modulus of elasticity, MPa
e	Error	f	Error function
h_c	Real contact depth, m	h_r	Residual depth after unloading, m
$h_{\max}$	Maximum contact depth, m	I	Property
K	Strength coefficient	n	Work hardening
P	Load, N	$P_{\max}$	Maximum load, N
R	Indenter radius, m	S	Unloading initial slope
h_a	Depth of circle of contact measured from specimen free surface, m	h	Depth, m
Greek symbols			
e	Strain	e_t	True strain
k	Stress ratio	Q	Contact half angle
s	Stress, MPa	s_1, s_2	Surface stresses, MPa
s_m	Normalized surface stress	s_t	True stress, MPa

*Corresponding author: R. Moharrami (Associate Professor)
E-mail address: r_ moharami@znu.ac.ir
http://dx.doi.org/10.22084/jrstan.2022.25733.1201
ISSN: 2588-2597

s_y	Yield stress, MPa		
Subscript			
app	Applied	*call*	Calculated

1. Introduction

Mechanical properties of materials determine their behavior against external factors such as loading. Although mechanical properties are intrinsic properties of materials, Doerner and Nix [1] showed that factors such as stress, temperature, radiation, and time could affect the mechanical properties. Periodic determination of structures' mechanical properties considering their loading is necessary to ensure engineering structures' health and efficiency in the future. Determination of materials' mechanical properties is conducted by destructive and non-destructive tests. Destructive tests, such as tensile test, provides more reliable results than non-destructive ones; however, they cannot be used for parts in service. Therefore, researchers have tried to use non-destructive tests for determining the parts' mechanical properties. In recent years, different techniques have been developed to determine the mechanical behavior of materials in a non-destructive way. One of these methods is IIT, which is efficient and powerful in determining some of the materials' properties, including elastic modulus, yield stress, and work hardening.

The principles of IIT are based on the indentation of a rigid body to a flexible body and examining its feedback. By indenting to depth h, the resistance force P is produced, and the *P-h* incremental loading curve can be drawn as Fig. 1. The unloading curve can also be drawn as the indenter returns to its initial height and by the gradual elimination of indentation. The most important data extracted from the figure is related to the unloading part, which include the initial slope of unloading section ($S = dP/dh$), contact depth (h_c), residual plastic displacement under the indenter after complete unloading (h_r), depth of circle of contact measured from specimen free surface (h_a) maximum depth (h_{max}), and maximum load (P_{max}). The properties of materials can be calculated with the use of mentioned initial information and methods which have been proposed for determining properties of materials by researchers [2].

The IIT has some advantages over other techniques, and different research works are still performed by industrial and academic centers to develop its applications and reduce the limitations of this method.

In 2005, a method for calculating elastic-plastic properties of homogeneous materials using the spherical indenter was developed by Lee et al. [3]. They determined the most optimum point for sampling beneath the indenter. Besides, they presented the indentation variables as a function of material properties by performing finite element (FE) simulation at the optimum point, and provided a novel numerical procedure of the IIT. In 2006, Kim et al. [4] utilized the IIT to determine materials' tensile properties and drew the strain-stress curve. The methodology includes examining the morphology of spherical indenter using the FE method. Then the plastic behavior of the material was formulated as a function of work hardening and the ratio of indentation depth to the indenter radius. The results were experimentally validated on 10 different materials. In 2011, Boschetto et al. [5] used the IIT to calculate the mechanical properties of steel parts.The C40 steel discs were cut from an extruded bar, and then successively machined by facing operation. Besides, the tungsten carbide indenters with diameters of 1mm and 2mm were used to calculate the yield strength and indentation pressure corresponding to each diameter. In 2019, Wang et al. [6] utilized the IIT to determine the Inc718 properties at high temperatures. They used the nanoindentation technique to determine the hardness, reduced modulus, and creeping parameters. They found that by increasing the room temperature up to 650°C, the modulus decreases by 22-26%. It is while that the corresponded reduction in hardness is 16-19%. In 2020, the neural networks and IIT were used to extract the elastoplastic properties of alloys with an acceptable precision by Lu et al. [7]. This method includes a multyfidelity procedure in which the deep-learning algorithms are trained to extract elastoplastic properties of metals and alloys from instrumented indentation results using multiple datasets

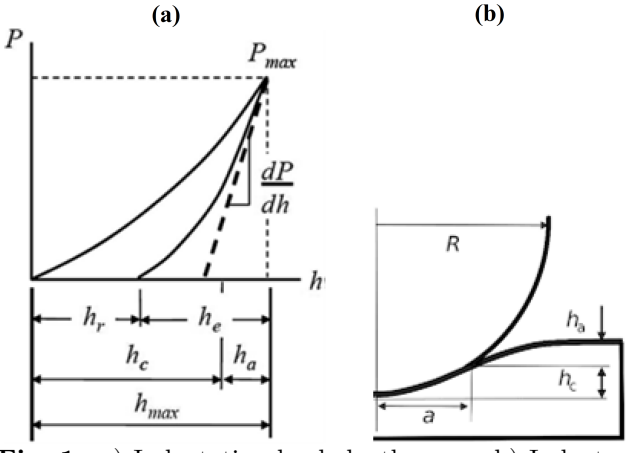

Fig. 1. a) Indentation load–depth curve, b) Indentation morphology [2].

In the studies mentioned above, the focus has been maily on development of techniques for determining the mechanical properties of materials using IIT by various methods. Accuracy and validation of this technique

in determining the mechanical properties is significant. Some researchers have directed their works toward examining possible errors and have focused their attentions on finding error sources, especially the effect of surface stresses on the results of properties' determination.

In 2004, Kese et al. [8] performed a research on the properties of soda-lime glass and found that stress has a significant effect on its mechanical behavior. Their results revealed that stress would decrease the elastic modulus. Besides, they have observed that hardness is independent of stress, except at the point exactly beneath the indenter where the stress is maximum. In 2006, Zhao et al. [9] found that a bulk material with a uniaxial residual compressive stress needs a higher force for indentation, while this force is less for a material with uniaxial residual tensile stress. This research was done both numerically and experimentally, and the maximum difference between results was less than 10%. In 2009, Huang et al. [10] used the nanoscratch and nanoindentation techniques to obtain residual stress's effect on the properties of thin films. They showed that the elastic modulus of the thin film declined from 95GPa in compressive stress of 235MPa to 86GP in tensile stress of 84MPa. In 2011, Khan et al. [11] investigated the effect of residual stresses on the nanoindentation of aluminum alloys in aerospace applications. They used the FE and experimental methods to calculate the maximum indentation load, loading curve's curvature, elastic recovery depth, indentation work, pile up, and surface contact. They showed that there is a linear relationship between these values and residual stress. In 2017, Skordaris et al. [12] performed a research on the PVD films and found that the properties, cohesion, brittleness, and adhesion of produced films are highly affected by residual stresses. The results showed that existence of stress has a considerable effect on the determination of the mechanical properties of the coatings under study.

Literature review shows that there is lack of quantitative studies on the effect of residual effects on the accuracy of the IIT technique in determining mechanical properties.

In this reaserch, the effect of non-equibiaxial surface stresses on the measurement accuracy of mechanical properties on A516, as a widely used steel in pressure vessels industry, was investigated. With this end in view, many simulations and some experimental tests were performed. The effect of different ratios of surface stresses $\kappa = \sigma_1/\sigma_2$ (≤ 1) and nomalized surface stress $|\sigma_{rn} = \sigma_2/\sigma_y|$ ($\leq$0.9) on the error of the IIT technique in determining the properties of the steel were obtained. Fig. 2 shows spherical indentation, two dimensional surface stresses and deviation in P-h curve. Due to the increasing use of IIT and the importance of reliability in its results, the results of this study can be used by other researchers.

2. Materials and Methods

The accuracy of mechanical properties estimation using Kim's model in different surface stresses state were numerically studied. With this end, a parametric three-dimensional FE model was developed, and consequently the mechanical properties estimation procedure by the indentation technique was simulated.

Due to the geometry and the contact details of the indenter and the specimen, a 10×10×10mm^3 cube FE model with symmetrical boundary conditions on the sides was considered as a quarter of the indented sample. The geometric model, as a deformable body, was meshed by the eight-node elements type C3D8R. Since the indentation area had large local deformations, to avoid simulation convergence errors, the elements of this area were considered to be finer than those of other areas. In this study, it was assumed that the surface stresses direction is definite and only the ball type indenter with diameter of 1/16in was used as the indentation tool. In the FE simulation, because of the strong hardness of the tool, relative to the sample, the ball indenter was modeled as a rigid body.

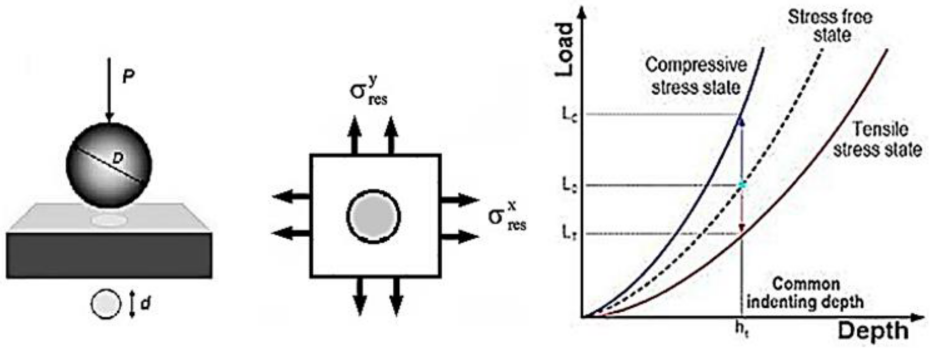

Fig. 2. Deviation in load–depth curve due to surface stresses [2].

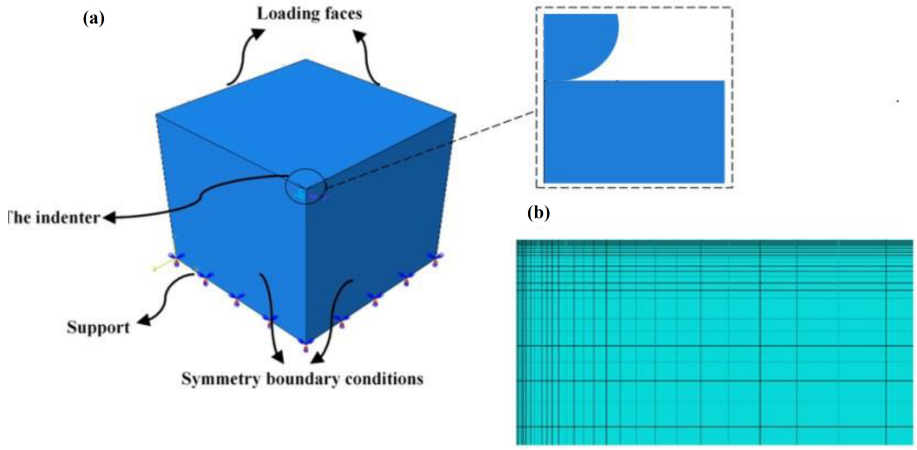

Fig. 3. The finite-element model: a) Boundary conditions, and b) The mesh beneath the indenter.

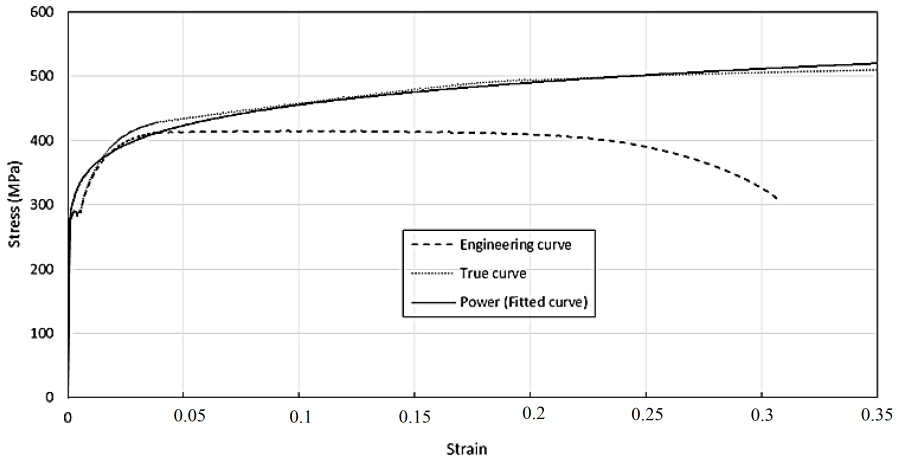

Fig. 4. True stress-strain curve with fitted curve used in simulation.

Fig. 3 depicts the geometric and meshed models with loading and boundary conditions. The biaxial compressive or tensile stress were applied to the model by applying pressure along the outer surface of the specimen, prior to the indentation as an alternative to the surface stresses state. The Coulombus friction law was employed between contact surfaces with the friction coefficient of 0.15 [13].

Tensile test was used to improve the accuracy of modeling the mechanical behavior of A516 steel in this study. Based on tensile test results, the behavior of the steel materials was considered to be elastic–plastic while isotropic strain hardening and elasic modulus, yield stress, and work hardening of the steel were considered to be 200GPa, 300MPa, and 0.1, respectively for all simulations. In this case, the stress-strain relationship of the material was defined as [14]:

$$\sigma = \begin{cases} E\varepsilon & \varepsilon \le \sigma_y/E \\ K\varepsilon^n & \varepsilon \ge \sigma_y/E \end{cases} \quad (1)$$

where, $K = \sigma_y(E/\sigma_y)^n$, E is Young's modulus, σ_y is yield strength, and the value of n is equal to the work hardening exponent. True stress-strain curve with used power law fitted curve are shown in Fig. 4.

In this study, in order to consider all the predicted cases, 33 simulations of instrumented indentation tests were performed. Material properties and stress conditions used in the simulations are presented in Table 1.

Table 1
Material properties and loading conditions.

0.1					Work hardening (n)
200GPa					Elastic modulus (E)
±0.9	±0.7	±0.5	±0.3	0	Normalized surface stress ($\sigma_{rn} = \sigma_2/\sigma_y$)
1	±0.75	±0.5	±0.25		Stress ratio ($\kappa = \sigma_1/\sigma_2$)
300MPa					Yield strength (σ_y)

In all simulations, the indentation depth was composed of ten $10\mu m$ steps, a total of $100\mu m$, which occured after each local unloading step. In the numerical analysis and simulation part of this reserch for all simulated cases, the force versus displacement variations, the P-h curve, were obtained. Fig. 5 shows a sample of extracted P-h curves from ball indentation simulation used for estimating mechanical properties by Kim's method.

3. Results and Discussions

Researchers have proposed different methods to determine material properties by analyzing the loading and unloading P-h curve. One of these methods is representative stress and strain [15] presented by Kim et al. [16]. In this method, multiple indentations in different indenting depths with a spherical indenter were used in order to calculate the desired material properties.

A second-order empirical equation, which is expressed in terms of n and h_{max}/R was employed to find the true stress and strain values [16].

An initial value for work hardening exponent, n, is taken into account so that an approximation of the real contact depth hc and the real contact surface Ac can be made. As shown in Fig. 6, by using relations (2) and (3), for each loading-unloading indentation in a certain depth, a single point on the true strain-stress curve is estimated [15].

$$\sigma_t = \frac{P}{3A_c} \tag{2}$$

$$\varepsilon_t = 0.14 \tan\theta \tag{3}$$

The constants "3" and "0.14" are plastic constraint factor and proportion coefficient respectively, and θ is the half-angle between contact surface and spherical indenter which is calculated from the indentation geometry [15].

By fitting the assumed power law of equation (1) into the calculated points, the complete stress-strain curve is created and the needed materials' properties, including elastic modulus (E), yield stress (σ_y), and work hardening (n), can be achieved [15]. If the new "n" is equal to the initial guess, the calculations are terminated, and the work hardening is obtained. Otherwise, the average of the calculated "n" and the initial guessed "n" is considered as the new "n", and the calculation is iterated.

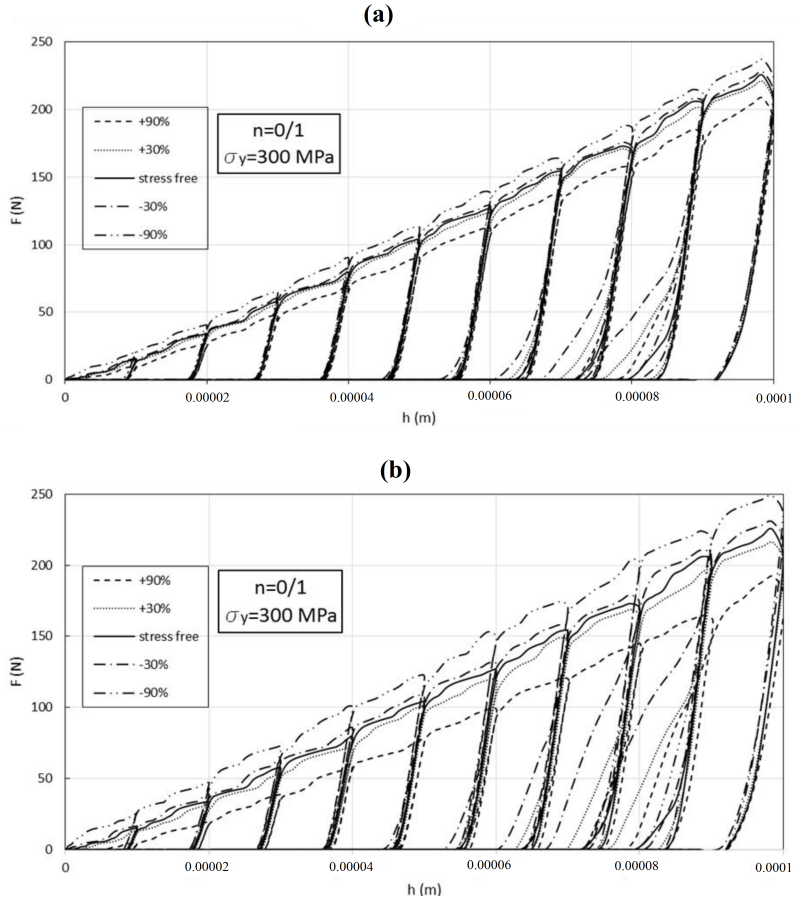

Fig. 5. Displacement-force curves of IIT simulation: a) Uniaxial for different normalized surface stresses, b) Biaxial (k=1) for different normalized surface stresses.

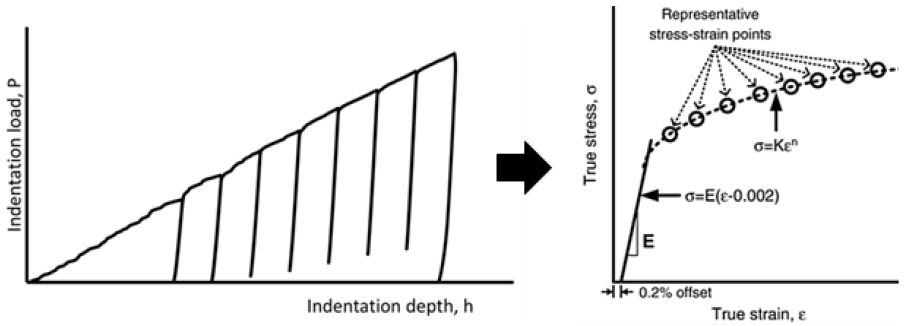

Fig. 6. Schematic stress-strain curve obtained by the Kim's method and IIT [15].

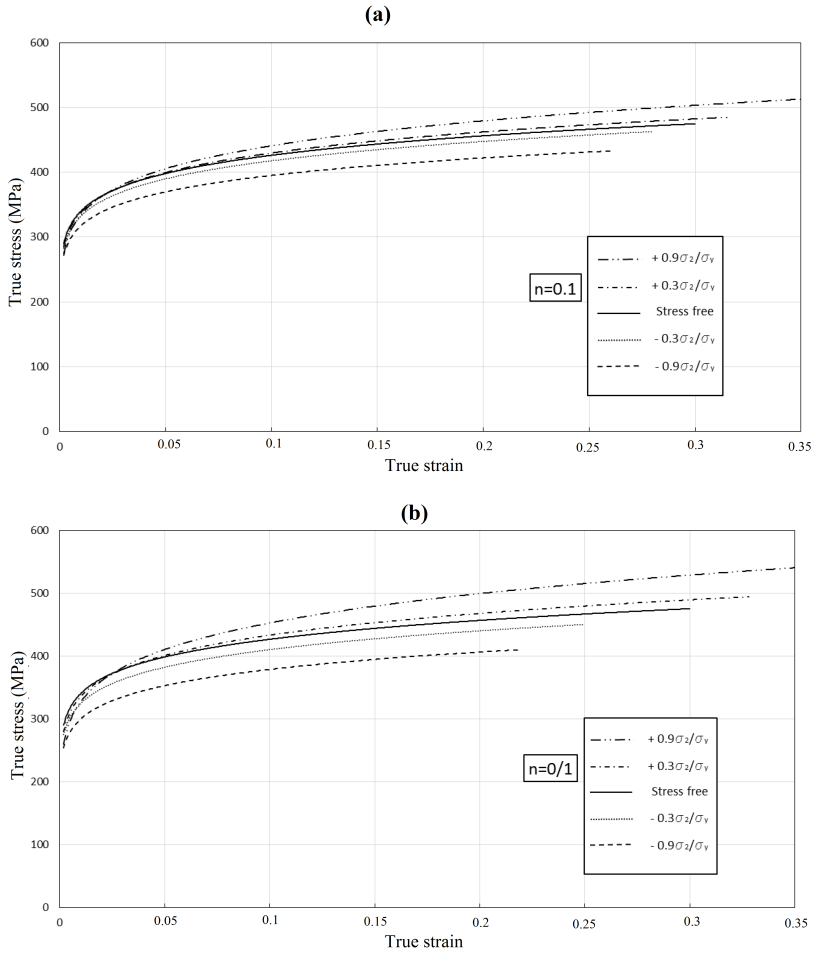

Fig. 7. The stress-strain curves simulated by IIT: a) Uniaxial for different normalized surface stresses, b) Biaxial ($\kappa = 1$) for different normalized surface stresses.

Since this method features a calculational algorithm, obtains data from different indentation depths, obtains the average results, it is more beneficial than other methods. Furthermore, another advatange is the minimum use of surface contact points.

Fig. 7 shows the stress-strain curves plotted by Kim method for a sample with different normalized surface stresses corresponding to the stresses shown in Fig. 5. It can be observed that by increasing the surface stresses, the calculational error increases and consequently the propertie's values deviate from the real value.

The inaccuracy of the mechanical properties calculated by Kim's model was quantitatively studied in different conditions as mentioned in Table 1. The error value in each case was obtained by comparing the calculated properties with the assumed properties as follows [17]:

$$\text{error} = \frac{I_{cal} - I_{app}}{I_{app}} \times 100 \tag{4}$$

where I_{app} is the real value of the property and I_{cal}

is the calculated value of the estimated property by Kim's method on the stressed sample. By calculating the errors, the deviation of properties from their real values is determined. The error of desired properties for different tensile and compressive surface stresses as well as the normalized surface stresses are presented in Table 2. As a result of Table 2, by moving from tensile stresses to compressive ones, the elastic modulus and yield stress increase, while the work hardening decreases.

The impacts of some parameters affecting Kim's model errors variation were studied using some 3D graphs. For further analysis, error variation was approximated by an appropriate function in each case study. Fig. 8 demonstrates the graphical results of the calculated error and two-dimensional surfaces fitted using the least-squares method. The general form of the obtained surface function as a third-degree two-variable equation is presented in Eq. (5), where x and y denote the normalized surface stress (σ_{rn}) and surface stress ratio (κ), respectively.

$$f(x,y) = ax + bx^2 + cx^3 + a'y + b'y^2 + c'y^3 + a''xy + b''x^2y + c''xy^2 + d \quad (5)$$

Table 2
Results of values of error calculations in A516 with surface stresses.

Applied stress		Calculated error for (n)	Calculated error for (σ_y)	Calculated error for (E)
$\sigma_{rn} = \sigma_2/\sigma_y$	$\kappa = \sigma_1/\sigma_2$	%	%	%
-0.9	0.25	-35	25	34
	0.5	-39	31	41
	0.75	-42	33	46
	1	-45	35	48
-0.7	0.25	-30	15	22
	0.5	-32	19	27
	0.75	-33	22	32
	1	-33	24	34
-0.5	0.25	-20	8	13
	0.5	-22	12	17
	0.75	-24	15	20
	1	-25	16	22
-0.3	0.25	-13	3	7
	0.5	-14	7	11
	0.75	-15	9	14
	1	-15	10	15
0	Equal	-5	1	2
0.3	0.25	15	-3	-7
	0.5	18	-7	-14
	0.75	20	-10	-17
	1	22	-11	-19
0.5	0.25	20	-10	-15
	0.5	28	-15	-22
	0.75	35	-19	-27
	1	38	-21	-29
0.7	0.25	40	-20	-30
	0.5	49	-26	-38
	0.75	55	-31	-44
	1	59	-32	-45
0.9	0.25	50	-38	-44
	0.5	63	-44	-53
	0.75	74	-49	-59
	1	78	-51	-63

a)

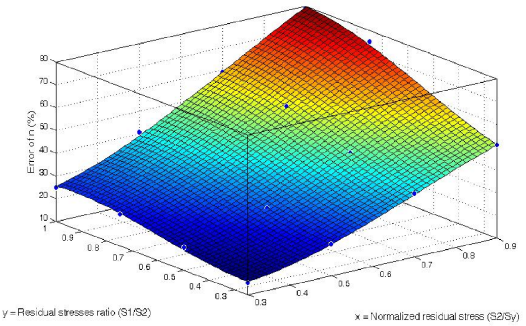

$f(x,y)=36.57-111.1x-69.58y+240.63x^2+60.6xy+130y^2-114.58x^3+5x^2y-20xy^2-69.33y^3$ ($R^2=0.9989$)

b)

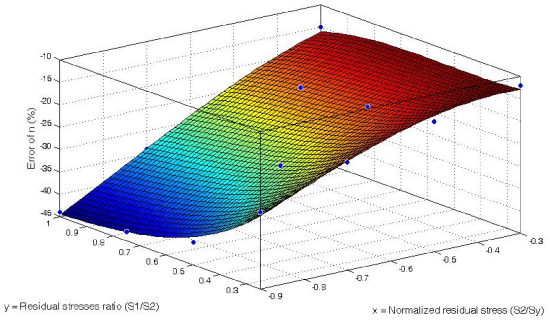

$f(x,y)=-28.93-100.66x+17.54y-131.25x^2+148.3xy+26y^2-46.88x^3+27.5x^2y-70xy^2-29.33y^3$($R^2=0.9823$)

c)

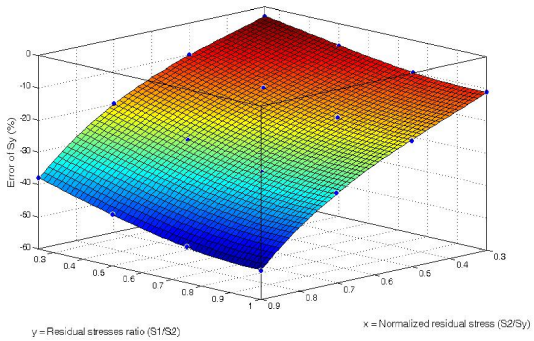

$f(x,y)=12.25-64.64x+5.38y+106.25x^2-44.5xy-26y^2-98.96x^3+17.5x^2y+10xy^2+18.67y^3$($R^2=0.9956$)

d)

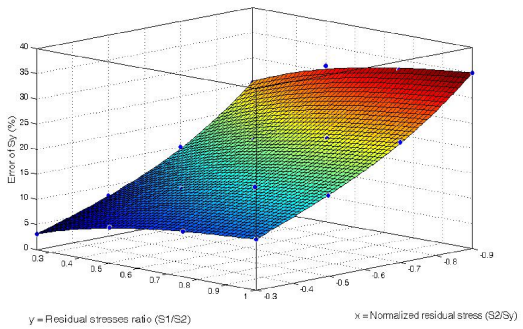

$f(x,y)=-10.63-30.83x+29.18y-37.5x^2-17xy-29.6y^2-41.67x^3-5x^2y+4xy^2+10.67y^3$($R^2=0.9799$)

e)

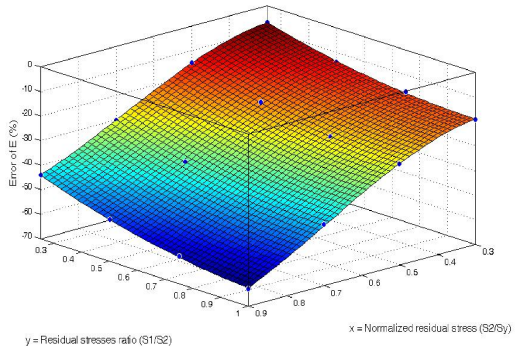

$f(x,y)=-15.42+139.19x-38.48y-315.63x^2-2xy+19.6y^2+156.25x^3-10x^2y+4xy^2+1.0168e-12y^3$($R^2=0.9921$)

f)

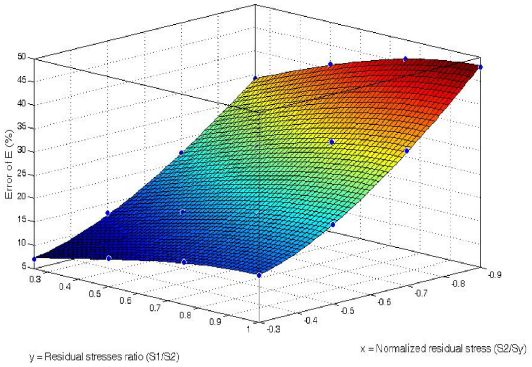

$f(x,y)=10.2+47.26x+0.138y+106.25x^2-22.7xy+20.4y^2+36.46x^3+7.5x^2y+14xy^2-13.33y^3$($R^2=0.9854$)

Fig. 8. a) Error of n in tensile stresses; b) Error of n in compressive stresses; c) Error of σ_y in tensile stresses; d) Error of σ_y in compressive stresses; e) Error of E in tensile stresses; f) Error of E in compressive stresses.

According to the results, it can be stated that in both compressive and tensile stresses, by increasing the surface stresses (σ_{rn}), and the surface stresses ratio (κ), the error in properties calculations increase. It was obsereved that in low amounts of σ_{rn} and κ, the error variation rate in tensile and compressive stress states are approximately equal. As σ_{rn} and κ get larger, the rate of error variation in tensile stress state has more increase comparing to the compressive stress state. As a result, in maximum tensile stresses the rate of error variation is 1.3, 1.5, and 1.7 times the rate of error variation in maximum compressive stresses for elastic modulus, yield stress, and work hardening, respectively. In tensile stresses the maximum error of elastic modulus,

yield stress, and work hardening for $\kappa = 1$ will be 63%, 51%, and 78%, respectively.

On the other hand, the corresponded errors in maximum compressive stresses errors are 34%, 25%, and 35%, respectively. The error variations are nearly linear until $\sigma_{rn} = \pm 30\%$, and then it becomes nonlinear and incremental until $\sigma_{rn} = \pm 90\%$. Nearly 50% error of ratio κ=1 occurs at ratio $\kappa = 0.25$. It means that the stress starting in the second dimension will lead to error up to 50%, and it is important that stress is considered in two dimensions.

4. Experimental Test and Verification

To validate the results of FE simulations, a cross-shaped sample made of A516 steel alloy was used. To obtain the real mechanical properties of the material, the heat treatment was performed to release the initial surface stresses and then standard tensile stress was conducted as mentioned before. The elastic modulus (E), yield stress (σ_y), and work hardening factor (n) obtained from the experimental tensile stress, as shown in Fig. 4, are represented in Table 3.

The sample was fixed in a special loading fixture, which was made according to [18]. The strain was applied to the sample by straining screws, and its value was measured by bounded strain gauge. Then, loading and unloading by the IIT equipment was performed on the sample by an indenter with a diameter of 1/16 in. During the test the loading rate was 0.2mm/min to fulfill quasi-static conditions. Fig. 9 shows the test fixture and the cross-shaped sample made of steel alloy.

Table 3
Results of standard tensile test on the steel sample.

Material	E (GPa)	σ_y (MPa)	n
A516	203	290	0.1

The sample was fixed in a special loading fixture, which was made according to [18]. The strain was applied to the sample by straining screws, and its value was measured by bounded strain gauge. Then, loading and unloading by the IIT equipment was performed on the sample by an indenter with a diameter of 1/16in. During the test the loading rate was 0.2mm/min to fulfill quasi-static conditions. Fig. 9 shows the test fixture and the cross-shaped sample made of steel alloy.

Some samples of loading conditions tests and their errors are shown in Table 4 where e_n, e_s and e_E are error of n, error of s_y and error of E, respectively.

These errors include the errors resulting from Eq. (5) obtained from simulation and the IIT error. In both cases, the results were compared with the properties applied from Table 1, and it can be seen that there is a good agreement between the results obtained from both methods.

The P-h curves obtained from simulation and experiment were compared and validated in the non-stressed conditions as shown in Fig. 10. Moreover, The stress-strain curves obtained from simulation and experiment were compared and validated by the tensile test curve in the non-stressed conditions as showed in Fig. 11.

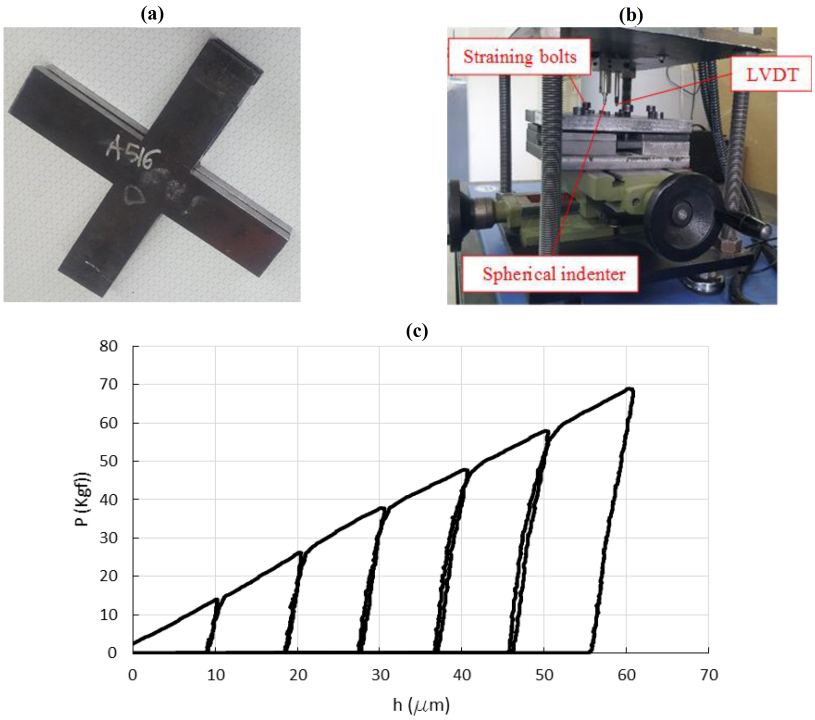

Fig. 9. a) Cross-shape sample; b) Test set; c) P-h Curve.

Table 4
Comparison of results of error function f(x,y) and IIT error.

Applied stress		Variables		Errors					
				IIT	FEM	IIT	FEM	IIT	FEM
s_1 (MPa)	s_2 (MPa)	s_2/s_y	k	e_n (%)	e_n (%)	e_s (%)	e_s (%)	e_E (%)	e_E (%)
-215	-222	-0.9	0.97	-48	-44	34	35	46	48
-172	-215	-0.87	0.8	-42	-42	30	32	45	44
105	175	0.71	0.6	52	51	-29	-29	-39	-41
196	245	0.99	0.8	82	83	-63	-62	-68	-65

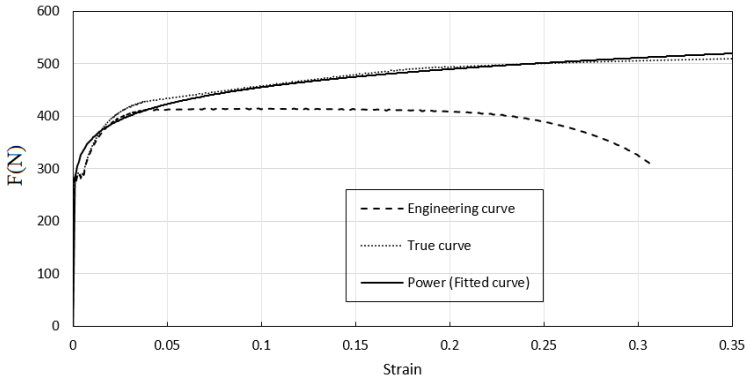

Fig. 10. Comparison of experimental IIT and simulation results in non-stressed conditions (P-h curve).

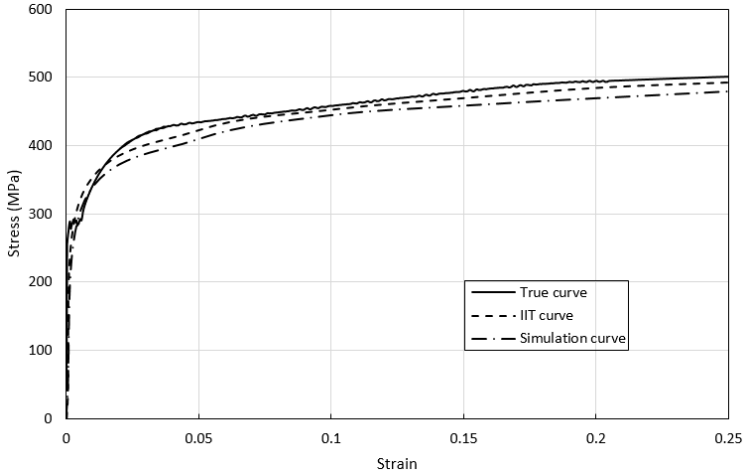

Fig. 11. Comparison of experimental IIT and simulation results with the tensile test curve in non-stressed conditions (Stress-strain curve).

5. Conclusions

In the present research, the materials' properties in general non-equibiaxial surface stress fields were estimated using both IIT and Kim's methods. With this end in view, 3D finite element simulations were performed to investigatethe effect of values and ratio of 2D surface stresses on the accuracy of preditions. It was observed that by increasing the normalized surface stresses (σ_{rn}), and the stress ratio (κ), the properties' error increased. Besides, the error slope in the tensile and compression ranges were not the same; such that the error variation rate in tensile was nearly two times as large as the compression. In tensile stresses, the maximum error of elastic modulus, yield stress, and work hardening for $\kappa = 1$ will be 63%, 51%, and 78%, respectively. On the other hand, the corresponded errors in maximum compressive errors were 34%, 25%, and 35%, respectively. The variations of error were nearly linear until $\sigma_{rn} = \pm 30\%$; then it became nonlinear and incremental until $\sigma_{rn} = \pm 90\%$. Nearly 50% error of ratio $\kappa = 1$ occurred at ratio $\kappa = 0.25$. It means that the stress starting in the second dimension

will lead to an error jump, showing the importance of considering stress in two dimensions..

Acknowledgement

This research was performed in Analysis, Measurement and Engineering of residual stresses (AMERS) Research laboratory at University of Zanjan. We thank the members of the research team for their cooperation and support.

References

[1] M.F. Doerner, W.D. Nix, A method for interpreting the data from depth-sensing indentation instruments, J. Mater. Res., 1(4) (1986) 601-609.

[2] A. Fischer-Cripps, Nanoindentation, 3 Edition, Springer New York, NY, (2011).

[3] H. Lee, J.H. Lee, G.M. Pharr, A numerical approach to spherical indentation techniques for material property evaluation, J. Mech. Phys. Solids, 53(9) (2005) 2037-2069.

[4] J.Y. Kim, K.W. Lee, J.S. Lee, D. Kwon, Determination of tensile properties by instrumented indentation technique: Representative stress and strain approach, Surf. Coat. Technol., 201(7) (2006) 4278-4283.

[5] A. Boschetto, F. Quadrini, E.A. Squeo, Extracting local mechanical properties of steel bars by means of instrumented flat indentation, Meas., 44(1) (2011) 129-138.

[6] H. Wang, A. Dhiman, H.E. Ostergaard, Y. Zhang, T. Siegmund, J.J. Kruzic, V. Tomar, Nanoindentation based properties of Inconel 718 at elevated temperatures: A comparison of conventional versus additively manufactured samples, Int. J. Plast., 120 (2019) 380-394.

[7] L. Lu, M. Dao, P. Kumar, U. Ramamurty, G.E. Karniadakis, S. Suresh, Extraction of mechanical properties of materials through deep learning from instrumented indentation, Proc. Natl. Acad. Sci., 117(13) (2020) 7052-7062.

[8] K.O. Kese, Z.C. Li, B. Bergman, Influence of residual stress on elastic modulus and hardness of soda-lime glass measured by nanoindentation, J. Mater. Res., 19(10) (2004) 3109-3119.

[9] M. Zhao, X. Chen, J. Yan, A.M. Karlsson, Determination of uniaxial residual stress and mechanical properties by instrumented indentation, Acta Mater., 54(10) (2006) 2823-2832.

[10] Y.C. Huang, S.Y. Chang, C.H. Chang, Effect of residual stresses on mechanical properties and interface adhesion strength of SiN thin films, Thin Solid Films, 517(17) (2009) 4857-4861.

[11] M.K. Khan, M.E. Fitzpatrick, S.V. Hainsworth, L. Edwards, Effect of residual stress on the nanoindentation response of aerospace aluminium alloys, Comput. Mater. Sci., 50(10) (2011) 2967-2976.

[12] G. Skordaris, K.D. Bouzakis, T. Kotsanis, P. Charalampous, E. Bouzakis, B. Breidenstein, B. Bergmann, B. Denkena, Effect of PVD film's residual stresses on their mechanical properties, brittleness, adhesion and cutting performance of coated tools, J. Manuf. Sci. Technol., 18 (2017) 145-151.

[13] L. Xiao, D. Ye, C. Chen, A further study on representativemodels for calculating the residual stress based on theinstrumented indentation technique, Comput. Mater. Sci., 82 (2014) 476-482.

[14] J. Yan, A.M. Karlsson, X. Chen, Determining plastic properties of a material with residual stress by using conical indentation, Int. J. Solids Struct., 44(11-12) (2007) 3720-3737.

[15] ISO, Metallic materials - Measurement of mechanical properties by an instrumented indentation test - Indentation tensile properties, in, ISO/TR 29381, (2008).

[16] S.H. Kim, B.W. Lee, Y. Choi, D. Kwon, Quantitative determination of contact depth during spherical indentation of metallic materials-A FEM study, Mater. Sci. Eng., A, 415(1-2) (2006) 59-65.

[17] R. Moharrami, M. Sanayei, Improvement of indentation technique for measuring general biaxial residual stresses in austenitic steels, Precis. Eng., 64 (2020) 220-227.

[18] Y.H. Lee, D. Kwon, Estimation of biaxial surface stress byinstrumented indentation with sharp indenters, J. Acta Mater., 52(6) (2004) 1555-1563.